

## Study of Current Decay Time during Disruption in JT-60U Tokamak

M.Okamoto 1), K.Y.Watanabe 2), Y.Shibata 3), N.Ohno 3), T.Nakano 4), Y.Kawano 4), A.Isayama 4), N.Oyama 4), G.Matsunaga 4), K.Kurihara 4), M.Goto 2), S.Sakakibara 2), M.Sugihara 5) and Y.Kamada 4) and JT-60 team 4)

1) Ishikawa National College of Technology, Ishikawa 929-0392, Japan

2) National Institute for Fusion Science, Toki 509-5292, Japan

3) Graduate School of Engineering, Nagoya University, Nagoya 464-8603, Japan

4) Japan Atomic Energy Agency, Ibaraki 311-0193, Japan

5) ITER Organization, Cadarache, France

e-mail contact of main author: okamoto@ishikawa-nct.ac.jp

**Abstract.** The plasma current decay time during initial phase of the radiation induced disruption in JT-60U tokamak is studied based on the plasma inductance and resistance estimated by experimental data. The features of this study are as follows; (i) the electron temperature profile during the current quench is estimated by the electron cyclotron emission (ECE) diagnostic systems and the measurement of He I line emission intensity ratios, and the plasma inductance is estimated by the CCS (Cauchy-Condition Surface) method with the magnetics [1]. (ii) in the radiation induced disruption plasmas, it is found that the time change rate of the plasma inductance during current quench is an important parameter as well as the plasma resistance to predict the current decay time.

### 1. Introduction

Disruption is one of the most crucial issues for the tokamak fusion reactors. Intense eddy currents and large halo currents generated during the current quench of the disruption induce large electromagnetic forces on the vacuum vessel and in-vessel components. The forces could be large enough to mechanically break the in-vessel components [2]. In order to estimate the force induced by eddy currents, precise prediction of plasma current decay time is important. The database for ITER (International Thermonuclear Experimental Reactor) [3] is established by using the current decay time  $\tau$  normalized by the plasma cross-sectional area  $S$ . The area-normalized  $\tau$  is induced by the L/R model based on a simple series circuit of the plasma resistance  $R_p$  and inductance  $L_p$ , where  $\tau$  can be described by  $L_p/R_p$ . In this model,  $\tau/S$  can be represented by  $(L_p/2\pi R_0)/\eta_p$ , it is little dependence on the device size and is strongly dependence on the electron temperature  $T_e$  and effective charge  $Z_{eff}$ , where  $R_0$  and  $\eta_p$  are the plasma major radius and resistivity, respectively. In the database, the lower bound on area-normalized  $\tau$ , which is taken as  $1.7 \text{ ms/m}^2$  [4], is used as the criterion value for design of ITER.

In order to experimentally evaluate the validity of the L/R model, very low  $T_e$  and  $Z_{eff}$  during current quench must be measured by the diagnostic system with high time resolution. D. G. Whyte and D.A.Humphreys had estimated the  $T_e$  and  $Z_{eff}$  during current quench using measurement of helium recombination radiation and reported the relation between the current decay time and classical resistivity [5,6]. However, the systematic analysis of the current decay time and electron temperature during current quench has not reported yet.

In this paper, the  $T_e$  profile during current quench is estimated by ECE diagnostic systems and measurement of He I emission intensity ratios. We verify the validity of L/R model using the initial phase of current quench of radiation induced disruptive plasma with  $\tau/S = 5 \sim 40 \text{ ms/m}^2$ . The measurement of  $T_e$  using ECE diagnostic systems in plasma core region is

possible during initial phase of slow current decay disruption in JT-60U Tokamak. In the edge region,  $T_e$  can be estimated by He I emission intensity ratio. The fundamental validity of the  $T_e$  measurement based on He I emission line intensity ratio was confirmed by comparing with  $T_e$  measurement by Langmuir probes in JT-60U [7] and NAGDIS-II [8], etc. According to ref. 7,  $T_e$  estimated by He I line intensity ratio is almost same with  $T_e$  by the probe within the factor of 2 and the former is systematically smaller than the latter.

We analyze 9 disruptive plasma shots with massive neon gas puffing. The safety factor, toroidal magnetic strength and NBI power just before current quench is not same among the shots. In addition, the time evolution of plasma inductance during current quench is focused, and relation between current decay time and plasma inductance is evaluated. The equilibrium calculation of MHD, which is calculated by the CCS method, is used to estimate the plasma inductance.

## 2. Model of Current Decay Time

If tokamak plasma is assumed to be represented by a simple series circuit consisting of  $R_p$  and  $L_p$ , the energy conservation equation is expressed as

$$\frac{1}{2}L_p I_p^2 + \int_0^t R_p I_p^2 dt = \int_0^t V_{ex} I_p dt + \frac{1}{2}L_{p0} I_{p0}^2, \quad (1)$$

where  $I_p$  and  $V_{ex}$  is the plasma current and the externally applied voltage,  $L_{p0}$  and  $I_{p0}$  is plasma inductance and current just before current quench, respectively. When Eq. 1 is transformed, it becomes the following circuit equation:

$$\frac{1}{2}\dot{L}_p I_p + L_p \dot{I}_p + R_p I_p = V_{ex}. \quad (2)$$

In the small tokamaks, the right-hand side of Eq. 2 cannot be neglect because the absolute value of the left-hand side of Eq. 2 is the same order of magnitude as the absolute value of  $V_{ex}$  [9]. On the other hand, the absolute value of  $V_{ex}$  is usually smaller than the left-hand side of Eq. 2 in the large tokamaks. This characteristic becomes more remarkable when device size becomes large. If  $R_p$  and  $L_p$  are constant in time, and  $V_{ex}$  can be neglect, the temporal evolution of  $I_p$  can be expressed by the following equation,

$$I_p = I_{p0} \exp(-t/\tau_{L/R}), \quad (3)$$

where  $\tau_{L/R} = L_p/R_p$  is the time constant of  $I_p$  decay. Equation 3 is valid when the current decay time is very short and plasma resistance is sufficiently large. When the current decay time can be approximated by  $\tau_{L/R} = L_p/R_p$ , the area-normalized current decay time  $\tau/S$  can be expressed as

$$\frac{\tau_{L/R}}{S} = \frac{L_p / 2\pi R_0}{\eta_p}, \quad (4)$$

where  $R_0$  is the plasma major radius,  $\eta_p$  is the plasma resistivity, and  $\eta_p = R_p S / 2\pi R_0$ .  $\tau_{L/R} / S$  has little dependence on the device size, because  $L_p$  is approximately proportional to  $R_0$ , and has a strong dependence on  $\eta_p$ , which is primarily determined by  $T_e$  and  $Z_{eff}$  in the classical Spitzer formula [10]. Thus, the database for ITER prediction is established in terms of the area-normalized current decay time  $\tau/S$  [3]. However, when  $R_p$  and  $L_p$  greatly change in time, Eq. 4 cannot be valid. Therefore, to verify the L/R model, it is necessary to measure  $L_p$  and  $R_p$  in time during current quench experimentally.

## 3. Experimental Result

### 3.1. Relation Between Area-normalized Current Decay Time and Plasma Resistivity

In this paper, we study the current decay time in the radiation induced disruption by the massive neon gas puffing. The typical waveform of plasma current  $I_p$ , line integrated electron density  $\bar{n}_e$ , plasma stored energy  $W_p$  and gas pressure of neon at disruption are shown in Fig. 1. After neon gas puffing, line integrated  $n_e$  is gradually increased and  $W_p$  is decreased, and then the current quench and rapid increase of line integrated  $n_e$  are observed.

We focus on the current decay during the initial phase of the current quench shown by the region enclosed by dotted line in Fig. 2(a), where  $I_p$  drops by 10%, because the  $T_e$  profile can be estimated by ECE diagnostic systems experimentally. The experimental current decay time during initial phase of current quench is defined by the following equation,

$$\tau_{100-90\%} = I_{p0} / (\Delta I_p / \Delta t), \quad (5)$$

where  $I_{p0}$  is the plasma current at the current quench start time. In this discharge, thermal quench is happened around at 12.089 sec and current quench is started about at 12.092 sec. From Fig. 2(c), it is found that  $T_e$  profile becomes flat at thermal quench and then returns to a peaked profile in the initial phase. In this phase,  $T_e$  in the core region is about 400 eV. Roughly speaking, because the optical thickness is small at  $T_e < 100$  eV, the sensitivity of ECE diagnostic systems becomes low and  $T_e$  at normalized minor radius  $\rho > 0.4$  cannot be estimated by ECE diagnostic systems. Here we use the He I emission intensity ratio method in

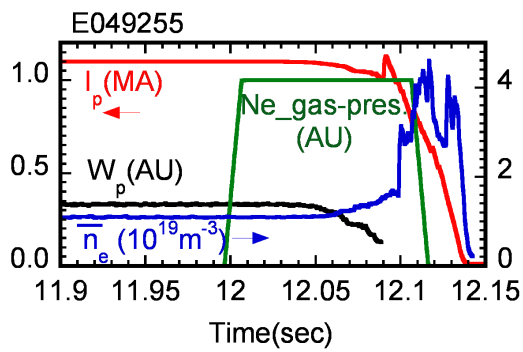


FIG. 1. The typical waveform of radiation induced disruption in JT-60U.

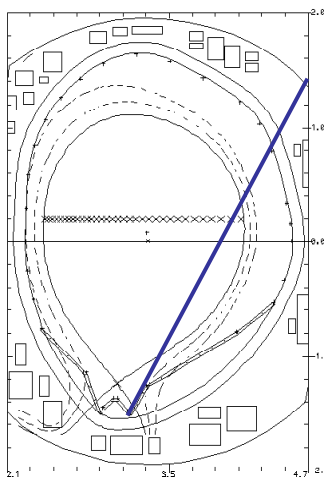


FIG. 3. Poloidal cross-section view of JT-60U plasma. Blue line means the line of sight for HeI spectroscopy.

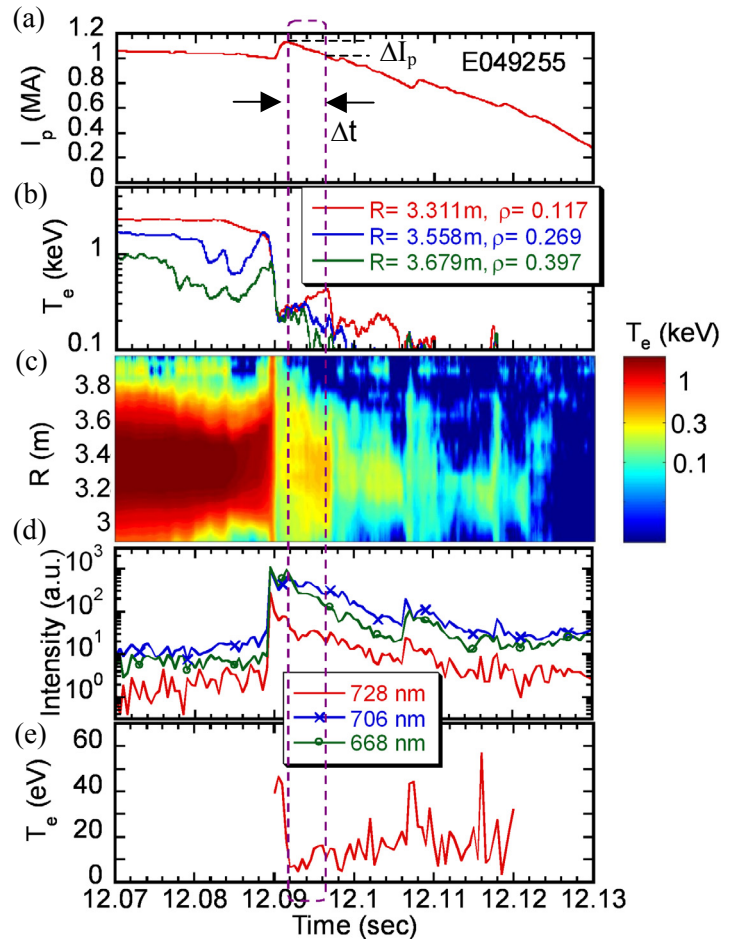


FIG. 2. The evaluation of (a) plasma current  $I_p$  and (b) electron temperature  $T_e$  measured by ECE diagnostic system, (c) major radial profile of  $T_e$ , (d) He I emission intensity and (e) electron temperature by using HeI emission Intensity ratios method.

the case that the estimated  $T_e$  by ECE is less than 100 eV. In order to measure the electron temperature, it is necessary to measure three He I lines at the same time of 667.8 ( $2^1P - 3^1D$ ), 706.5 ( $2^3P - 3^3S$ ) and 728.1 nm ( $2^1P - 3^1S$ ) respectively. A spectrometer equipped with three band pass interference filters makes it possible to measure the time evolution of  $T_e$  with a sufficient time resolution. Figure 3 shows the line of sight for measurement of ECE (crosses) and He I emission intensity (solid line). The He I emission intensity is measured from the outer divertor region though the edge region of  $\rho > 0.7$ . Figure 2(d) and (e) shows the measurement result of He I emission intensity and the estimated electron temperature. From Fig. 2(d), it is found that He I emission intensity increase rapidly about at  $t = 12.089$  sec, which is the thermal quench start time. Before the thermal quench, the He I emission mainly comes from the divertor region because He neutrals only exist in this region. On the other hand, after the thermal quench, the He I emission comes from the edge region also because  $T_e$  rapidly decreases in the whole region due to the thermal quench. Since the measurement value of He I emission intensity is the integration value on line of sight and the measurement position of  $T_e$  estimated by He I emission intensity ratio cannot specify, its position is assumed  $\rho = 0.7$ .

Figure 4 shows the assumed  $T_e$  profile using measurement values of ECE diagnostic systems and He I emission intensity ratios method at  $t = 12.094$  sec. In this figure, opened circles and cross mean  $T_e$  estimated by ECE systems and He I spectroscopy, respectively. The  $T_e$  of  $\rho = 0.4 - 0.7$  and  $0.7 - 1$  is assumed by a linear function. Unfortunately, we cannot obtain the accurate profile of the plasma resistivity because the plasma effective charge  $Z_{eff}$  cannot be measured in the initial phase of current quench. In order to speculate  $Z_{eff}$ , we use the ionic fraction data of neon calculated by Arnaud and Rohtenflug [11]. If the mixing ratios of deuterium and neon gas are 9 : 1, 7 : 3 and 1 : 1 and these ratios are uniform in space, the calculation results of  $Z_{eff}$  and  $\eta_p$  are shown in Fig. 5. The  $\eta_p$  is calculated by Spitzer formula and assumed  $Z_{eff}$ . In Fig. 5, the upper and lower values of error bar are values calculated using assumptions of D : Ne = 1 : 1 and 9 : 1, respectively. The values of  $Z_{eff}$  in the core and edge region are about 7 and 2, respectively.

In order to investigate the relation between area-normalized  $\tau$  and plasma resistivity, we

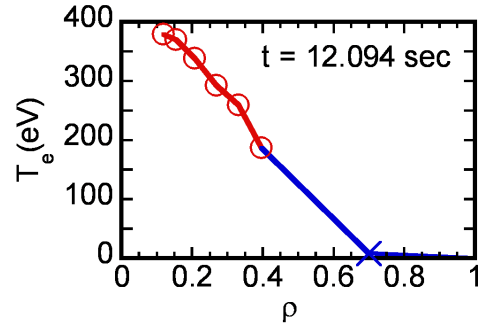


FIG. 4. Profile of electron temperature measured by ECE systems and He I spectroscopy at  $t = 12.094$  sec.

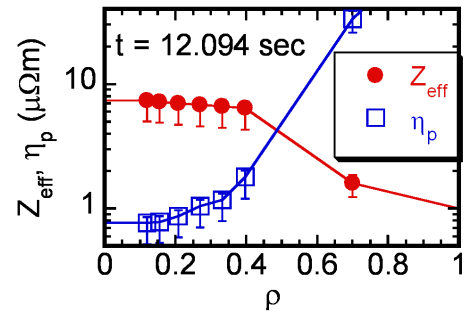


FIG. 5. Profile of plasma effective charge and resistivity at  $t = 12.094$  sec. The effective charge is calculated using the assumption of D : Ne = 9 : 1, 7 : 3 and 1 : 1.

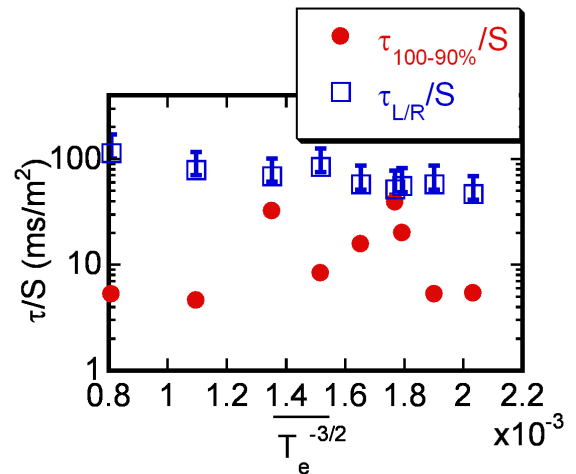


FIG. 6. The area-normalized current decay time as a function the area-averaged  $T_e^{-3/2}$

use area-averaged  $T_e^{-3/2}$  calculated by

$$\overline{T_e^{-3/2}} = S / \sum (\Delta S / T_e^{-3/2}), \quad (6)$$

where  $S$  is the plasma cross-section area. This value is proportional to the area-averaged plasma resistivity  $\bar{\eta}_p$  with  $Z_{eff} = 1$ . The area-averaged  $\eta_p$  can be estimated by  $\eta_p$  profile in Fig.5 and following equation,

$$\bar{\eta}_p = S / \sum (\Delta S / \eta_p). \quad (7)$$

The relation between area-normalized  $\tau$  and area-averaged  $T_e^{-3/2}$  is shown in Fig. 6. In Fig. 6, the  $\overline{T_e^{-3/2}}$  is calculated by Eq. 6 and the profile of time averaged  $T_e^{-3/2}$  during the initial phase of current quench. In the similar way,  $\tau_{L/R}/S$  is calculated by Eq. 4, 7 and the profile of time averaged  $\eta_p$ . The upper and lower values of error bar of  $\tau_{L/R}/S$  are values calculated using assumptions of D : Ne = 9 : 1 and 1 : 1, respectively. It is found that the experimental area-normalized  $\tau$  is independent of the area-averaged  $T_e^{-3/2}$  and the prediction area-normalized decay time  $\tau_{L/R}/S$  calculated from L/R model is much longer than the experimental value, especially in the case of small experimental values. It seems that this result means the L/R model does not verify and  $L_p$  is not constant and greatly changes in time during initial phase of current quench.

### 3.2. Time Evolution of Plasma Inductance using CCS Method

We use the CCS method using magnetic sensor signals due to evaluate the temporal evolution of plasma inductance and plasma shape. This method can obtain the exact analytical solution

based on the boundary element method using a static Maxwell equation with a Green function in a toroidal axisymmetric region [1]. In a case of several magnetic sensors, we can obtain the approximate solution of the magnetic field and flux according to the accuracy and the number of sensors. It was confirmed that the error of Shafranov lambda value calculated by this method is less than 0.1 in JT-60U measurement systems, which have 12 magnetic coils and 15 magnetic flux loops. Figures 7 show the results calculated by using a Cauchy condition (both Dirichlet and Neumann conditions) on a hypothetical surface. From Fig. 7(d), because  $R_0$  is almost constant and  $S$  changes a little, plasma column hardly moves in the initial phase of current quench. In Fig. 7(b), since the plasma internal inductance  $l_i$  is decrease rapidly around at  $t = 12.089$  sec, the current density profile becomes flat at thermal quench. This result is consistent of the measurement of  $T_e$  using ECE systems as Fig. 1(c). After the flattening of current density profile, it is found that  $l_i$  much

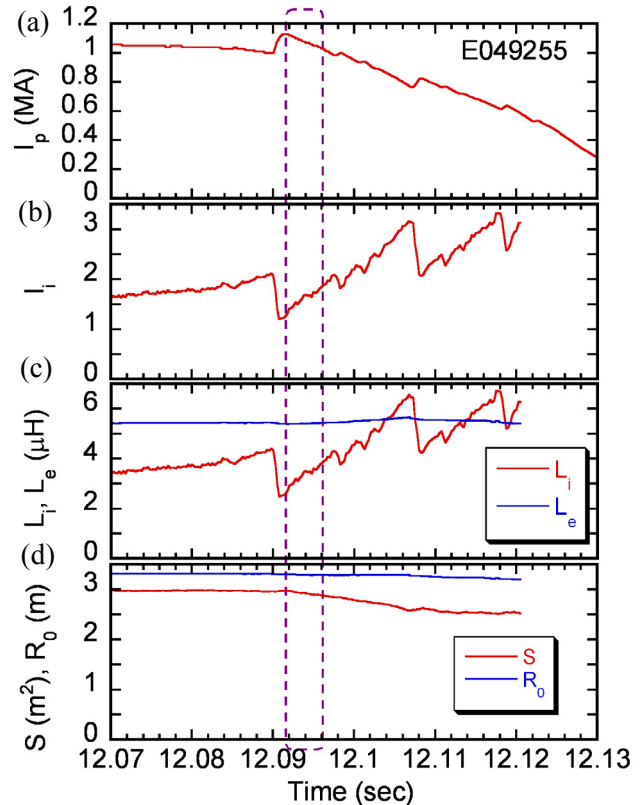


FIG. 7. The evolution of (a) plasma current, (b) plasma internal and inductance, (c) plasma internal and external inductance and (d) plasma cross-section and major radius evaluated by CCS method.

increases in time. This result is also consistent of ECE measurement results because  $T_e$  profile changes peaked profile in Fig.1 (c). In Fig. 7(c), the plasma internal and external inductance is calculated by following equations,

$$L_i = \mu_0 R_0 I_i / 2, \quad (8)$$

$$L_e = \mu_0 R_0 (\ln 8 R_0 / a - 2), \quad (9)$$

where  $a$  is the plasma minor radius. It is found that time change rate of  $L_i$  is much larger than that of  $L_e$  and time change rate of  $L_p$  is mainly determined by that of  $L_i$ .

Figure 8 shows the comparison of absolute value of  $R_p$ ,  $L_p$  and time change rate of  $L_p$  in the initial phase of current quench. The  $R_p$  and  $L_p$  are calculated by  $R_p = 2\pi R_0 \bar{\eta}_p / S$  and  $L_p = L_i + L_e$ , respectively and these values are time averaged values during initial phase of current quench. It is found that the absolute value of time change rate of  $L_p$  is the same order of magnitude as that of  $R_p$  or much larger than  $R_p$  in the short current decay time region. In addition, the experimental current decay time is dependent on the time change rate of  $L_p$ . Therefore, it is necessary that the time change rate of  $L_p$  is taken into account in the circuit equation in order to accurately predict the current decay time in the initial phase of current quench.

### 3.3. Current Decay Model during Initial Phase of Current Quench

From Eq. 2 with  $V_{ex} = 0$ , we obtain the following equation:

$$\frac{\dot{I}_p}{I_p} = -\frac{\dot{L}_p / 2 + R_p}{L_p}. \quad (10)$$

To simplify the equation, if  $\dot{L}_p = \Delta L_p / \Delta t$ ,  $R_p$  and  $L_p$  is constant in time, the prediction current decay time  $\tau_{model2}$  can be represented by

$$\tau_{model2} = \frac{L_p}{\Delta L_p / 2\Delta t + R_p}. \quad (11)$$

Figure 9 shows the comparison of prediction times, which are calculated by L/R model and Eq. 11, and experimental time. As shown in Fig.8, although  $\tau_{L/R}$  is much larger than the experimental decay time in the short decay time region,  $\tau_{model2}$  is same order of magnitude as experimental decay time in some disruptive discharges and experimental decay time increases with  $\tau_{model2}$ . The time evolution of plasma inductance is almost determined by the change rate of plasma internal inductance. The above result indicates that the change rate of the plasma internal inductance associated with current profile plays a key role to predict the precise current decay time during initial phase of current quench in JT-60U radiation induced disruptive plasmas. Here it should be noted the absolute value of  $\tau_{model2}$  is not quite same as that of the experimental decay time in Fig. 9. This result is mainly from an estimation error of plasma inductance because the

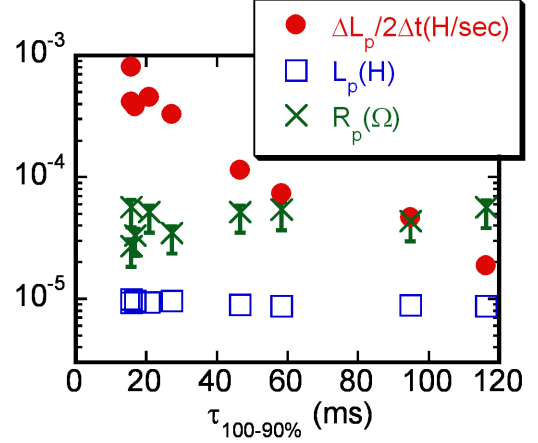


FIG. 8. The plasma resistance  $R_p$ , the plasma inductance  $L_p$  and the time change rate of the plasma inductance as a function of current decay time.

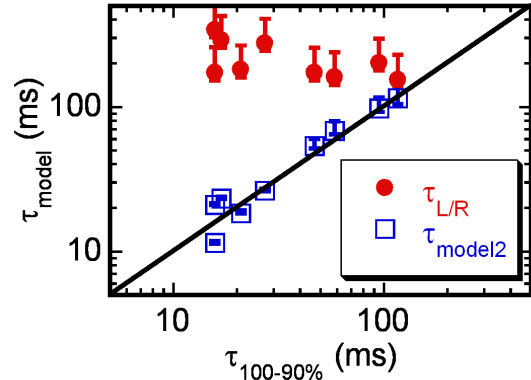


FIG.9. The comparison of the experimental value and the model prediction value of current decay time in initial phase of current quench.

dependency of experimental decay time on  $T_e$  would be smaller than that on time change rate of  $L_p$ . As the candidate of the estimation error of inductance, the neglect of the eddy current during current quench in the CCS method should be considered in near future.

#### 4. Summary

We have investigated the current decay time using the initial phase of JT-60U radiation induced disruptive discharges experimentally. The plasma resistance is estimated by ECE diagnostic systems and He I emission intensity ratios and the plasma inductance is calculated by CCS method using magnetic sensor signals. It is experimentally confirmed that the area-normalized decay time in initial phase of current quench is independent of the electron temperature and decay time calculated from L/R model is larger than the experimental decay time. This result indicates that the plasma inductance greatly changes in time.

The time change rate of plasma inductance estimated by CCS method is the same order of magnitude as plasma resistance or much larger than plasma resistance. So, we consider a new model of the current decay time, which is taking the time evolution of the plasma inductance into account in the circuit equation. The prediction of the current decay time predicted by the new model is strongly dependent on the experimental time and these absolute values are almost same. Therefore, the change rate of the plasma internal inductance plays a key role to predict the precise current decay time during initial phase of current quench in JT-60U tokamak. Here, it should be noted the new prediction value is not quite same as the experimental value. As the reason of this result, the neglect of the eddy current during current quench in the CCS method is considered. As the future works, we should improve the CCS method by taking the eddy current effect into account and make sure the validity of the CCS method through the direct measurement of the current profile like the MSE. In this paper, we have just investigated the validity of L/R model. As a next step, we should investigate what dominate the time change rate of the plasma inductance. This is one of our future subjects.

#### References

- [1] Kurihara K., Fusion Eng. Des., **51-52** (2000) 1049.
- [2] Masaki K., Ando T., Kodama K., Arai T. et al., J. Nucl. Mater. **220-222** (1995) 390.
- [3] Progress in the ITER Physical Basis, Nuclear Fusion **47** (2007) S171.
- [4] Wesley J.C., Hyatt A.W., Strait E. J. and Schissel D. P. et al., Proceedings of 21st IAEA Fusion Energy Conference, Chengdu, 16-21 Oct. (2006) IT/P1-21.
- [5] Whyte D.G., Humphreys D.A. and Taylor P. L., Phys. Plasma **19** (2000) 4052.
- [6] Humphreys D.A. and Whyte D.G., Phys. Plasma **19** (2000) 4057.
- [7] Kubo H., Goto M. and Takenaga H. et al., J. Plasma and Fusion Res., **75** (1999) 945.
- [8] Kajita S., Ohno N. and Takamura S. et al., Physics of Plasmas, **13** (2006) 013301.
- [9] Okamoto M., Ohno N. and Takamura S., J. Plasma and Fusion Res., **3** (2008) 006-1.
- [10] Spitzer L. and Härm R., Physical Review **89** (1953) 977.
- [11] Arnaud M., Rothenflug R., Astron. Astrophys. Suppl. Ser. **60** (1985) 425.